AIP | Journal of Applied Physics

Electrical control of the spin polarization of a current in "pure-carbon" systems based on partially hydrogenated graphene nanoribbon

Yan-Dong Guo, Xiao-Hong Yan, and Yang Xiao

Citation: J. Appl. Phys. **113**, 244302 (2013); doi: 10.1063/1.4811716
View online: http://dx.doi.org/10.1063/1.4811716
View Table of Contents: http://jap.aip.org/resource/1/JAPIAU/v113/i24
Published by the AIP Publishing LLC.

Electrical control of the spin polarization of a current in "pure-carbon" systems based on partially hydrogenated graphene nanoribbon

Yan-Dong Guo,[1] Xiao-Hong Yan,[1,2,a)] and Yang Xiao[1]
[1]*College of Science, Nanjing University of Aeronautics and Astronautics, Nanjing 210016, China*
[2]*College of Electronic Science and Engineering, Nanjing University of Posts and Telecommunications, Nanjing 210046, China*

(Received 29 March 2013; accepted 7 June 2013; published online 25 June 2013)

Controlling a spin current by electrical means and eliminating the use of ferromagnetic contacts becomes a focus of research in spintronics, as compared with conventional magnetic control methods, electrical one could reduce the dimensions and energy consumption of integrated devices. Inspired by recent progress of controlling the hydrogenation on graphene [Xie *et al.*, Appl. Phys. Lett. **98**, 193113 (2011)], we investigate the electronic structure and spin-current transport of partially hydrogenated zigzag graphene nanoribbon (ZGNR) with various hydrogenation geometries, through first-principles calculations. It is found that for ZGNR in ferromagnetic edge-coupling state, near-edge hydrogenation would suppress the magnetization on the edge of ZGNR, and lower down the transmission around E_F to zero except two peaks, which reside discretely on both sides of E_F with opposite spins. Based on this feature, we propose and demonstrate a three-terminal device, where the spin polarization of the current can be modulated by gate voltage (V_g) to vary from (almost) 100% to −100%, which could serve as a perfect electrically-controlled "pure-carbon" dual-spin filter. Especially, the spin polarization varies gradually with V_g, so a current with any ratio of spin-up to spin-down electron numbers can be achieved. Moreover, the influences of ZGNR width and hydrogenation-region length on the system's performance are also discussed and a large range of ZGNR configurations are found to be suitable for the application of such a device. © *2013 AIP Publishing LLC*.
[http://dx.doi.org/10.1063/1.4811716]

I. INTRODUCTION

Spintronics is an emerging field for future nanoelectronics.[1–4] The control of a spin current is one of the key points in this area. To reduce the dimensions and energy consumption of integrated devices, there is considerable interest in controlling the spin current by electrical means and eliminating the use of ferromagnetic (FM) contacts.[5] Due to the spontaneous magnetic moments at edges, zigzag graphene nanoribbon (ZGNR) exhibits great application potential in spintronics.[6,7] It has been reported that the ZGNR under antiferromagnetic (AFM) state could be modulated by an electric field to become half-metallic and operate as a spin filter.[6] However, at finite temperature or in the presence of a current, this AFM state is found to be unstable.[8–10]

Recently, the progress in controlling the hydrogenation of graphene makes it possible to design various geometries of hydrogenation regions on graphene (e.g., rectangular one),[11,12] which exhibit interesting magnetic properties.[13–16] Creating zigzag edges and hydrogenation are two metal-free ways to obtain magnetic moments on graphene, and both of their structures can be viewed as "pure-carbon" systems. With the continuous miniaturization, silicon device would soon encounter scientific and technical limits. Due to the superior electrical properties, carbon-based materials are considered to be one of the most promising candidates for future nanoelectronics.[17] In particular, pure-carbon devices involve carbon (and hydrogen) atoms only. They are easy to fabricate, compatible with a variety of carbon components, and chemically inert, realizing large-scale integration and stable operation. Thus, pure-carbon systems are quite beneficial for the device application. As the two ways to obtain magnetic moments on graphene mentioned above are compatible in experiment, it is necessary to study the effect of their interplay on the magnetism, and especially on the spin-current transport, when they are combined together. Despite extensive investigations have been carried out on the spin-current transport of ZGNR, a study on such a system is still lacking.

In this paper, we focus on the FM state of ZGNR, which could be stabilized by a magnetic field,[18] and study the magnetism, together with the spin-current transport, of the partially hydrogenated ZGNRs. To explore the systems more accurately, density functional theory calculations combined with nonequilibrium Green's function are preformed. It is found that, the near-edge hydrogenation would suppress the magnetic moments on zigzag edges. In particular, the electronic transmission near E_F could be lowered down to zero, but two peaks still remain, residing discretely on both sides of E_F with opposite spins. Through the analysis of transmission eigenchannels, we illustrate the mechanism of such suppression of transmission. Moreover, based on this transmission feature, we propose a gate-controlled dual-spin filter, and demonstrate its performance under a finite bias, where the spin polarization (SP) of the current could be electrically modulated between (almost) 100% and −100%, realizing the

a)Electronic mail: xhyan@nuaa.edu.cn

electrical control of spin current in a "pure-carbon" system. As the SP varies gradually with V_g, a current with any ratio of spin-up to spin-down electron numbers can be obtained. Furthermore, the influences of the ZGNR width and the hydrogenation-region length are also discussed, and a large range of ZGNR configurations, which are suitable for the application of such a device, are revealed.

II. COMPUTATIONAL METHOD

The calculations are carried out by the Atomistix Toolkit package,[2,19] which is based on the combination of density functional theory and nonequilibrium Green's function. We use the mesh cutoff energy of 150 Ry, and $1 \times 1 \times 100$ k-point mesh in the Monkhorst-Park scheme.[20] The Perdew-Zunger parameterization of local spin-density approximation (LSDA) is used as the exchange-correlation function.[21] Double zeta plus polarization basis set is chosen to be the local numerical orbitals. To prevent the interaction with adjacent images, supercell with sufficient vacuum spaces (more than 10 Å) is employed. For the three-terminal device, the dielectric material is 3.2 Å thick with dielectric constant of $10\,\varepsilon_0$, and ZGNR is positioned 1.5 Å above it. For clarity, N denotes the width of ZGNR, i.e., the number of zigzag chains across the ribbon.

III. RESULTS AND DISCUSSIONS

For ZGNR, the ground state is in AFM coupling for the two edges. By applying transverse electric field, the ZGNR in AFM state is found to become half-metallic.[6] However, at finite temperature or in the presence of a current, this AFM state would become unstable.[8–10] Slightly above it in energy, there is an FM state, with parallel magnetic configuration for the two edges.[18,22] It is found that a magnetic field could stabilize the FM state.[18] Thus, it will be more practical to make the device operate in this state.[23,24]

Here, we take the infinite 5-ZGNR [Fig. 1(a), for N-ZGNR, N denotes the width of ZGNR, i.e., the number of zigzag chains across the ribbon] as an example to show the electronic structure of ZGNR in FM state. Figures 1(b) and 1(c) give out its bandstructure and density of states (DOS), respectively. From them, one finds there are two bands across E_F, which result in a finite DOS at E_F and contribute to the conductance. Thus, the 5-ZGNR is conducting.[18] Interestingly, two flat parts of the bands (around -0.3 and 0.2 eV) for spin up and down contribute to two peaks in DOS, respectively, which reside discretely on both sides of E_F. From another point of view, the infinite ZGNR in Fig. 1(a) can be considered as a two-terminal device, i.e., a finite 5-ZGNR contacted with two semi-infinite 5-ZGNR leads. For such a system, its transmission spectrum under zero bias ($V_L = V_R$) are shown in Fig. 1(d). As one finds, there are two transmission peaks, which are contributed by the corresponding DOS peaks. And for the other energies, the transmission coefficients are 1.0 for both spin up and spin down. In our DFT+NEGF scheme, the transmission coefficient $T(E)$ is the sum of the transmission eigenvalues at energy E, which represent the probabilities that the incoming wave function transports through the scattering region in corresponding

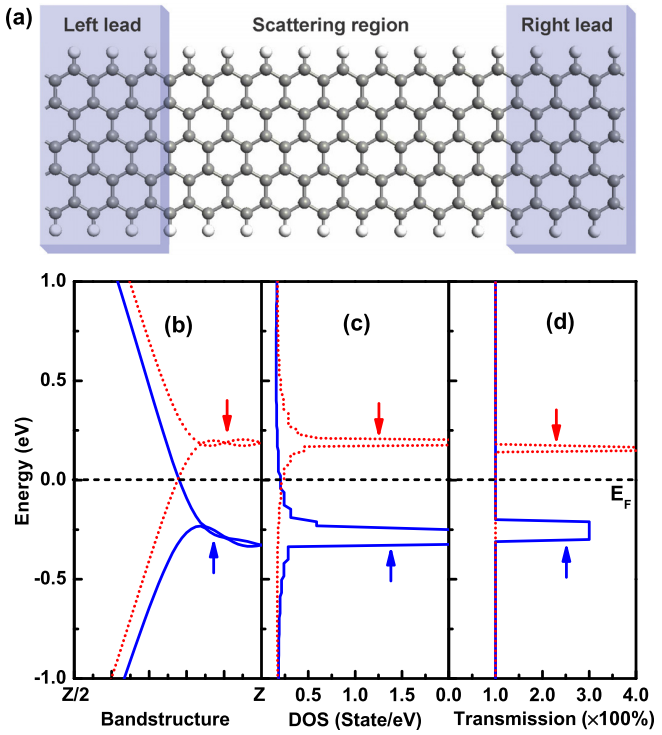

FIG. 1. (a) Schematic illustration of two-terminal device constructed by infinite 5-ZGNR. (b)–(d) The corresponding spin-dependent bandstructure, density of states, and transmission spectrum for 5-ZGNR in FM state, respectively. The zero of energy is set to be the Fermi level, which is defined as the average of the Fermi levels of the two leads.

eigenchannels. For each eigenchannel, the maximal conductivity is $G_0 = 2e^2/h$, i.e., the conductance quantum. At some energies, there are more than one eigenchannels, so the transmission there may exceed 1.0, e.g., the two transmission peaks in Fig. 1(d).

As a spin-polarized current is related to the electronic structures, here we give out the spin charge density magnetization (i.e., up-spin charge density minus down-spin charge density) of the 5-ZGNR, shown in the left part of Fig. 2(a). Apparently, the magnetic charge density is largely localized at the edge atoms. From the edges to the center, the density magnetization decays rapidly. As well known, for graphene nanoribbons, it is the edge states that dominate the electronic transport. So, modifying the edge states is a convenient and good way to modulate the electronic transport of ZGNR. Next, we partially hydrogenate the 5-ZGNR with different geometries of hydrogenation, and find out how the hydrogenation affects the edge magnetization and the spin-current transport.

Here, we partially hydrogenate the 5-ZGNR with several typical geometries, shown in the left and right panels of Fig. 2 [only the scattering region is shown and its left and right parts are connected with semi-infinite bare 5-ZGNRs like Fig. 1(a)]. The shaded region indicates the area passivated by hydrogen atoms (the adjacent carbon atoms are hydrogenated in the opposite sides). The configuration in Fig. 2(h) is taken as an example to illustrate the structural optimization method [see Fig. 2(i) and the caption] and show the three-dimensional view of the geometry [Fig. 2(j)]. In the middle of Fig. 2, the corresponding transmission spectrum for each hydrogenation

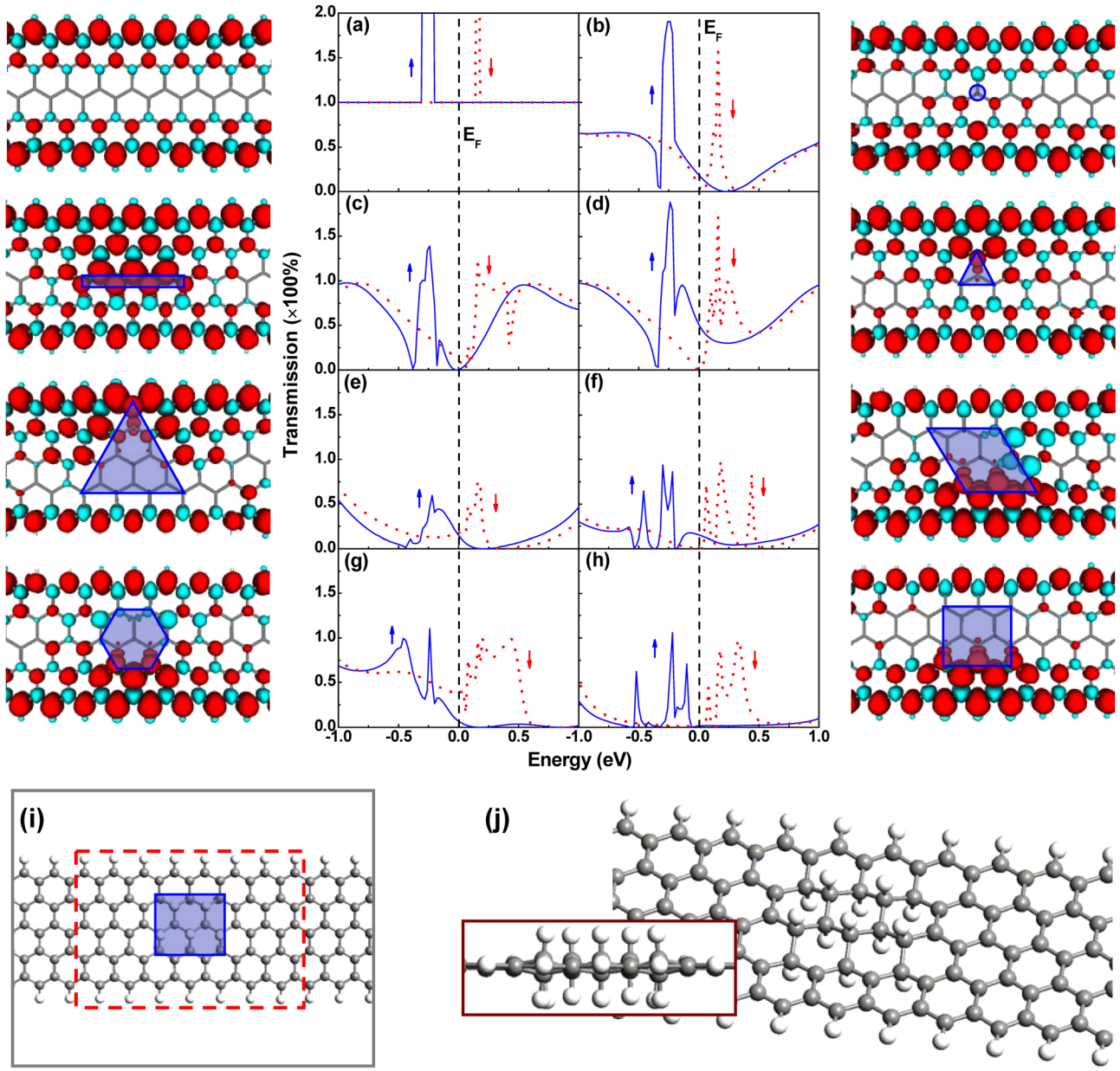

FIG. 2. (a)–(h) Spin-dependent electronic transmission spectra for (a) bare and (b)–(h) partially hydrogenated 5-ZGNRs with different hydrogenation geometries. The left and right panels show the corresponding configurations and their isovalue surfaces of the spin charge density magnetization (i.e., up-spin charge density minus down-spin charge density). Red (dark) and blue (light) represent positive (spin-up polarized) and negative (spin-down polarized) values, respectively, with the isovalue of $1.0 \times 10^{-2}\,e/Å^3$. The isovalue surfaces exhibit spherical geometries around atoms, where large size indicates large magnetization (near-edge atoms) and small size indicates small magnetization (inner atoms). For clarity, balls for atoms are not shown, and the shaded region is passivated by hydrogen atoms. (i) Take the configuration in (h) as an example to show the structural optimization. The scattering region shown in (i) is considered to be a periodic configuration for optimization, and the unit cell is shown by the gray and solid box. During the optimization, the atoms outside the red and dashed box are frozen, meanwhile, the atoms within that box (including the shaded region) are fully relaxed until all the forces are less than 0.02 eV/Å. This would stabilize the whole hydrogenation area (shaded region), including its edges. After optimization, the left and right sides of the scattering region are contacted with semi-infinite GNR electrodes to calculate the transport properties. (j) The three-dimensional and enlarged views of the configuration in (h).

case is shown [Fig. 2(a) is for the bare 5-ZGNR]. Comparing Figs. 2(b)–2(h) with Fig. 2(a), one finds hydrogenation will induce a suppression of the transmission around E_F for both spins, no matter what geometry of the hydrogenation is. For graphene, carbon atoms are all in a plane, with sp^2 hybridization. The electrons which are not take part in bonding are shared by all atoms, and it is those mobile electrons that contribute to electronic transmission.[25] Saturating graphene with hydrogen atoms would change the bond type of carbon from sp^2 to sp^3, converting graphene to graphane, which is highly insulating.[15] As a result, the increase in relative area of insulating graphane (or in other words, the decrease in mobile electrons) due to hydrogenation suppresses the transmission spectrum.[14] For the magnetization around the hydrogenation region, its variation (increase or decrease) is closely related to the shape and the edge of the hydrogenation area. To understand it completely, more details should be considered and a systematic study needs to be done. In this work, we restrict our studies to the influence of hydrogenation on the edge magnetization and the spin current.

From Fig. 2, we can see, if the hydrogenation region is far away from the edges, it tends to enhance the magnetization on the ribbons, such as Figs. 2(b), 2(c), and 2(d). In contrast, if the edge of hydrogenation region, especially for a long linear edge, is quite close to the zigzag edge of ZGNR, it will suppress the magnetization, e.g., the lower edge of triangular hydrogenation in Fig. 2(e) and the upper edges in Figs. 2(f) and 2(h). Obviously, compared with other cases, the transmission spectra in Figs. 2(f) and 2(h) are suppressed the most. For these two hydrogenation geometries, they both have long linear hydrogenation edges, which are close to the edges of ZGNR. Interestingly, although the transmission is lowered down to almost zero, the two peaks mentioned above still remain (one for spin up and one for spin down). But they have been split into several peaks. It should be noted that for each peak energy, the transmission for another spin is very small, e.g., in Fig. 2(h) around 0.25 eV, the spin-up transmission is quite small under the spin-down peak. Based on this feature, we propose that, with a gate electrode, the peak could be shifted to the Fermi level, and then the current will be dominated by the sign of its spin, where a "pure-carbon" electrically-controlled dual-spin filter could be realized.

For this purpose, the rectangular configuration in Fig. 2(h) is the most suitable candidate, because of the large contrast of the transmission between up and down spins at the peak energies. However, around 0.25 eV in Fig. 2(h), although the spin-up transmission is quite small under the spin-down peak, there is still some leakage transmission. In Fig. 3(e), we give out the enlarged view for that part. This leakage will no doubt reduce the efficiency of the spin filter. We have calculated its spin-filter efficiency after gate shifting, and it only reaches to 80% (not shown).

To further increase the spin-filter efficiency, we next try to suppress the leakage transmission. For the hydrogenation cases in Fig. 2, the position of the shaded region is not equal relative to the two edges of ZGNR, such as the configuration of Fig. 2(h). It is more clearly shown in Fig. 3(a). From Fig. 3(a), we can see the magnetizations for the top and bottom edges of the hydrogenation region are quite different. Easy to know, hydrogenating another line of carbon atoms under the bottom of the shaded region would further suppress the magnetization and transmission. Naturally, we enlarge the hydrogenation region from the configuration of Fig. 3(a) to that of Fig. 3(b). The corresponding magnetization and transmission spectrum are shown in Figs. 3(d) and 3(f), respectively. Compared with Fig. 3(e), one finds the leakage transmission under the peak of Fig. 3(f) is greatly suppressed (see the enlarged insets in the two figures).

To further understand the suppression effect, we pick up three typical energy points (0, −0.28, and 0.15 eV, corresponding to E_F and the two peaks) to see the change of electron transmission eigenchannels due to the hydrogenation in Fig. 3(b). Table I gives out the transmission eigenchannels and corresponding eigenvalues for those energies before and after hydrogenation. For E_F (0 eV), there are two eigenchannels (one for spin up and one for spin down) before hydrogenation, and they are both totally opened (1.0). After hydrogenation, they are almost totally blocked, where the transmission becomes zero at E_F. For the energy −0.28 eV, there are three spin-up and one spin-down eigenchannels for bare 5-ZGNR, which are all totally opened. After hydrogenation, the spin-down channel is almost blocked. But some of the spin-up channels are still partially opened. Thus, the spin-up peak around −0.3 eV remains [Fig. 4(b)], and this mechanism also works for the spin-down peak.

As mentioned above, for the two peaks, if one of them could be shifted to E_F, the SP direction of current would be determined by the sign of its spin. Thus, controlling the SP

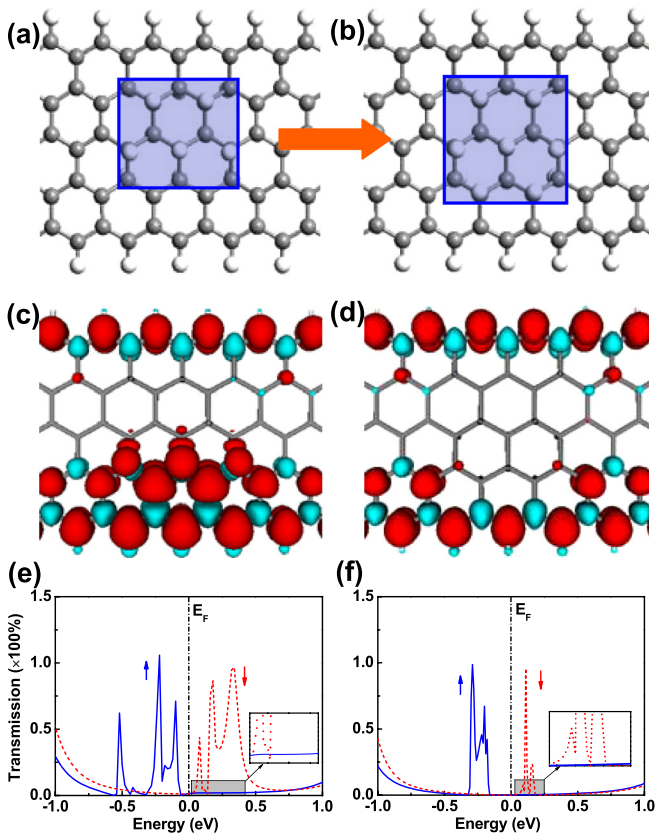

FIG. 3. Left and right panels show the structures of 5-ZGNRs with two different hydrogenation geometries [(a) and (b)], corresponding spin charge density magnetizations [(c) and (d)] and transmission spectra [(e) and (f)].

TABLE I. Transmission eigenchannels and the corresponding eigenvalues for bare [Fig. 1(a)] and partially hydrogenated 5-ZGNR [Fig. 3(b)].

	−0.28 eV		0 eV		0.15 eV	
Structure	↑	↓	↑	↓	↑	↓
Bare[a]	1.0	1.0	1.0	1.0	1.0	1.0
	1.0					1.0
	1.0					1.0
						1.0
						1.0
Add H[b]	0.30	0.0061	0.00039	0.0020	0.0027	0.060
	0.029					0.031
	0.000055					0.0018
						0.00014
						0.0000013

[a]Corresponding to the configuration in Fig. 1(a).
[b]Corresponding to the configuration in Fig. 3(b).

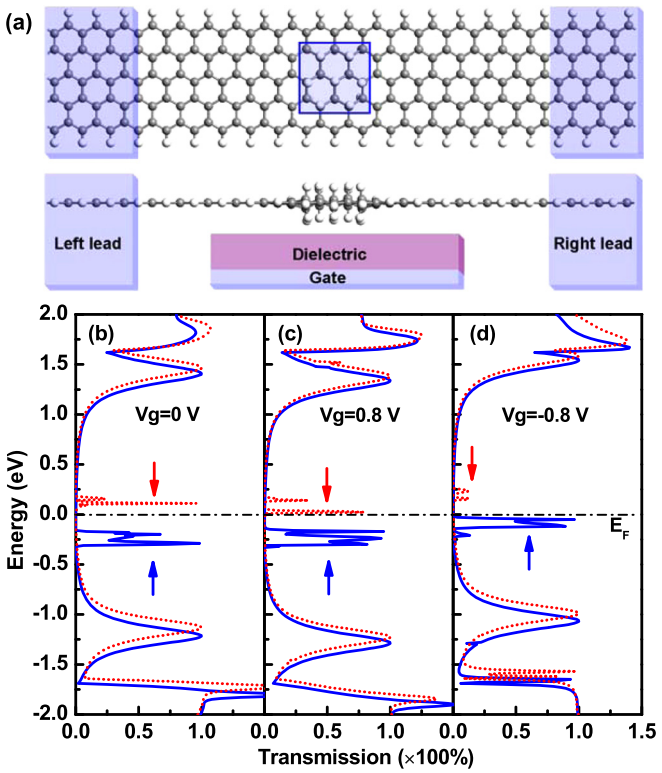

FIG. 4. (a) Schematic illustration (top and side views) of three-terminal ZGNR device with rectangular hydrogenation in FM state. The carbon atoms within the middle shaded region are passivated by hydrogen atoms. (b)–(d) The corresponding spin-dependent transmission spectra for $V_g = 0$, 0.8, and -0.8 V, respectively.

equals to shifting the transmission peaks to E_F. In a three-terminal device, a gate voltage is found to be able to shift the energy levels up or down relative to E_F.[26] We here introduce a gate electrode and construct a three-terminal device shown in Fig. 4(a). To confirm the shifting effect, Figs. 4(c) and 4(d) show the transmission spectra for $V_g = 0.8$ and -0.8 V under zero bias, respectively. Apparently, a positive (or negative) V_g could lower down (or raise up) the energy levels in the scattering region, and either of the two peaks could move to E_F. By applying a source-drain bias (V_b), the peaks would enter into the integration window of current and contribute to it, as the current for each spin is obtained according to the function

$$I(V_b, V_g) = \frac{e}{h}\int_{\mu_R}^{\mu_L} T(E, V_b, V_g)[f(E-\mu_R) - f(E-\mu_L)]dE,$$

where $T(E, V_b)$ is the transmission spectrum, $f(E-\mu_{L,R})$ is the fermi function for the left (right) lead, and $\mu_{L,R}$ is the lead's chemical potential. For the bias between two leads, it is $V_b = (\mu_L - \mu_R)/e$. And the Fermi level of the whole system is defined as the average of the chemical potentials of the two leads.

As a demonstration, a bias of 10 mV between left and right leads is applied to the device. The corresponding spin-dependent currents are given out in Fig. 5(a). For spin-up current (I_{up}), it is almost zero when $V_g = 0$, as the transmission coefficient for spin-up is zero at E_F [Fig. 4(a)]. When V_g increases, I_{up} remains to be zero. This is because a positive

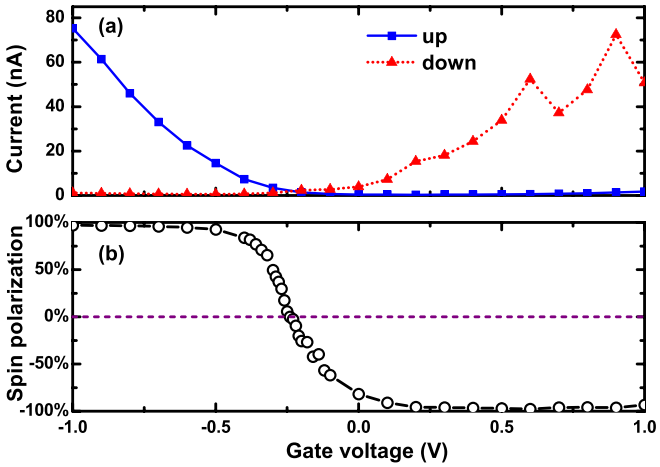

FIG. 5. (a) The spin-dependent currents under bias of 10 mV between left and right leads vary with V_g for the device shown in Fig. 4. (b) The corresponding spin polarization of the current varies with V_g.

V_g would shift the transmission spectrum down, but there is no spin-up peak above E_F for a large energy region. On the contrary, a negative V_g can shift the spin-up peak up to E_F. So the current increases when V_g goes to a proper negative value. For spin-down current, it could be interpreted in a similar way. The two currents exhibit opposite variation trend and intersect at about -0.25 eV [see Fig. 5(a)].

We here define the SP of a current as $[(I_{up} - I_{down})/(I_{up} + I_{down})] \times 100\%$, and Fig. 5(b) shows the variation of SP with V_g. Surprisingly, the polarization can range from almost 100% to -100%, i.e., completely spin-up polarized to completely spin-down polarized. This three-terminal device can achieve the same effect as the ferromagnets under magnetic field to switch the SP direction of a current. However, our device is realized through electrical means, which will operate faster and be more convenient to integrate into nanoelectronic devices. Moreover, it cannot only switch the SP from 100% to -100%, but also achieve any SP ratio between 100% and -100%, as the polarization changes gradually against V_g from 100% to -100%. That is to say, we can get the current with any ratio of spin-up to spin-down electron numbers. We believe this feature is very useful for the development of future spintronic devices. And the device is constructed by graphene, which is a promising candidate for future nanoelectronic applications. In addition, the structure consists of carbon and hydrogen atoms only, which can be seen as a "pure-carbon" system. This kind of structure could be fabricated in experiment.[14,15]

In the above device, the key point is the particular transmission spectrum after partial hydrogenation. For a large energy region around E_F, the transmission is zero except two peaks near E_F, which reside discretely on both sides of E_F with opposite spins. In theory, a structure with similar transmission spectrum could be used to construct such a device. Next, we check for the performances of the device when we change the hydrogenation-length and ZGNR width. First, we change the length of the hydrogenation region by increasing and shrinking it, shown in Figs. 6(a) and 6(b), respectively. Compared with Fig. 4(b), increasing length would suppress transmission and lower down the peak, whereas shrinking

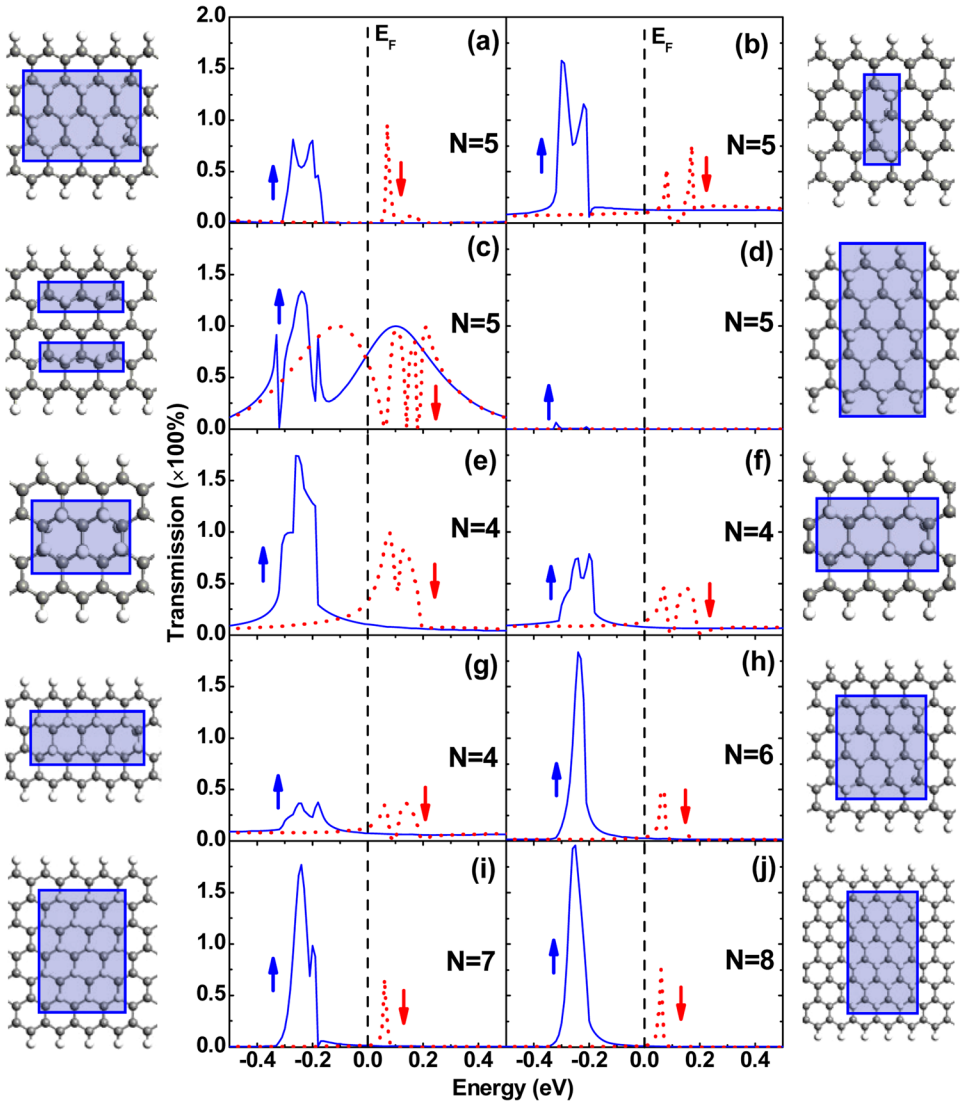

FIG. 6. The spin-dependent transmission spectra for two-terminal N-ZGNR device with different widths (N) and different hydrogenation geometries. Left and right panels give out corresponding structures [only the scattering region is shown, and its left and right are connected with semi-infinite bare ZGNRs like Fig. 1(a)]. The carbon atoms within the shaded region are passivated by hydrogen atoms. (a)–(d) for $N = 5$, (e)–(g) for $N = 4$, and (h)–(j) for $N = 6$, 7, and 8, respectively.

length would weaken the suppression and the peak goes up (especially for the spin-up peak). But for shorter length in Fig. 6(b), under each peak, there is leakage transmission for another spin. So it is not suitable for the device, as the SP cannot be complete due to the leakage. Then, we change the region by shrinking and increasing the width, shown in Figs. 6(c) and 6(d). Apparently, shrinking the region width will weaken the suppression effect on the edge states, and finite transmission arises around E_F [Figure 6(c)]. While, the configuration in Fig. 6(d) makes the two peaks disappear, which means overfull suppression can be induced by complete hydrogenation.

Now, we check the effect of ZGNR width. Fig. 6(e) shows the transmission spectrum for 4-ZGNR. Although the length of hydrogenation region is the same like $N = 5$ case in Fig. 4(a), large leakage transmission appears due to the change of ZGNR width. To suppress the leakage, we increase the region length, shown in Figs. 6(f) and 6(g). One finds the peaks are lowered down from Figs. 6(e) to 6(g), but the leakage not. We attribute this to the too small width of 4-ZGNR, which makes the hydrogenation region narrower, and the interaction between edges could not be suppressed completely [like the $N = 5$ case in Fig. 6(c)]. To confirm it, we give out the transmission spectra for ZGNR with larger widths, i.e., $N = 6$, 7, and 8 [Fig. 6(h)–6(j)]. For them, the leakage disappears. In brief, not only 5-ZGNR, but also wider ZGNRs ($N \geq 5$) with suitable hydrogenation region all can be used for the proposed device.

IV. CONCLUSION

In summary, based on first-principles calculations, we study the magnetization and spin-dependent electronic transport of partially hydrogenated ZGNR in FM state with different hydrogenation geometries, and propose a graphene-based three-terminal device, to realize the electrical control of spin polarization of a current. Without ferromagnetics, it is a "pure-carbon" system, and the spin polarization could vary from almost 100% to −100%. The suppression of electronic transmission by near-edge hydrogenation, the two spin-dependent transmission peaks near E_F, and the shifting of energy levels by V_g, are the key mechanisms for the device's operation. Moreover, the influences of the ZGNR width and the hydrogenation-region length are also discussed, and a large range of ZGNR configurations, which are suitable for the application of such a device, are revealed.

ACKNOWLEDGMENTS

This work is supported by the National Natural Science Foundation of China (NSFC10874089 and NSFC51032002), the key project of National High Technology Research and Development Program of China (2011AA050526), the Funding of Jiangsu Innovation Program for Graduate Education (CXZZ11_0190), and the Fundamental Research Funds for the Central Universities (NS2012005 and NS2012064).

[1]D. Awschalom and M. Flatt, Nat. Phys. **3**, 153 (2007).
[2]M. Brandbyge, J.-L. Mozos, P. Ordejón, J. Taylor, and K. Stokbro, Phys. Rev. B **65**, 165401 (2002).
[3]A. Brataas, Nature **452**, 419 (2008).
[4]S. Ciraci, S. Dag, T. Yildirim, O. Gulseren, and R. T. Senger, J. Phys. Condens. Matter **16**, R901 (2004).
[5]C. Chappert, A. Fert, and F. Van Dau, Nature Mater. **6**, 813 (2007).
[6]Y.-W. Son, M. L. Cohen, and S. G. Louie, Nature **444**, 347 (2006).
[7]W. Y. Kim and K. S. Kim, Nat. Nanotechnol. **3**, 408 (2008).
[8]N. D. Mermin and H. Wagner, Phys. Rev. Lett. **17**, 1133 (1966).
[9]D. A. Areshkin and C. T. White, Nano Lett. **7**, 3253 (2007).
[10]Z. Li, H. Qian, J. Wu, B.-L. Gu, and W. Duan, Phys. Rev. Lett. **100**, 206802 (2008).
[11]I.-S. Byun, D. Yoon, J. S. Choi, I. Hwang, D. H. Lee, M. J. Lee, T. Kawai, Y.-W. Son, Q. Jia, H. Cheong *et al.*, ACS Nano **5**, 6417 (2011).
[12]P. Sessi, J. R. Guest, M. Bode, and N. P. Guisinger, Nano Lett. **9**, 4343 (2009).
[13]L. Xie, X. Wang, J. Lu, Z. Ni, Z. Luo, H. Mao, R. Wang, Y. Wang, H. Huang, D. Qi *et al.*, Appl. Phys. Lett. **98**, 193113 (2011).
[14]R. Balog, B. Jørgensen, L. Nilsson, M. Andersen, E. Rienks, M. Bianchi, M. Fanetti, E. Lægsgaard, A. Baraldi, S. Lizzit *et al.*, Nature Mater. **9**, 315 (2010).
[15]D. C. Elias, R. R. Nair, T. M. G. Mohiuddin, S. V. Morozov, P. Blake, M. P. Halsall, A. C. Ferrari, D. W. Boukhvalov, M. I. Katsnelson, A. K. Geim, and K. S. Novoselov, Science **323**, 610 (2009).
[16]M. Yang, A. Nurbawono, C. Zhang, Y. P. Feng, and Ariando, Appl. Phys. Lett. **96**, 193115 (2010).
[17]P. Avouris, Z. Chen, and V. Perebeinos, Nat. Nanotechnol. **2**, 605 (2007).
[18]F. Muñoz Rojas, J. Fernández-Rossier, and J. J. Palacios, Phys. Rev. Lett. **102**, 136810 (2009).
[19]Atomistix ToolKit version 11.8, QuantumWise A/S (www.quantumwise.com).
[20]H. J. Monkhorst and J. D. Pack, Phys. Rev. B **13**, 5188 (1976).
[21]J. P. Perdew and A. Zunger, Phys. Rev. B **23**, 5048 (1981).
[22]D. Gunlycke, D. Areshkin, J. Li, J. Mintmire, and C. White, Nano Lett. **7**, 3608 (2007).
[23]F. Liu, Y. Li, X. Liu, and J. Kang, Appl. Phys. Lett. **99**, 243503 (2011).
[24]T. Ozaki, K. Nishio, H. Weng, and H. Kino, Phys. Rev. B **81**, 075422 (2010).
[25]A. Savchenko, Science **323**, 589 (2009).
[26]H. Song, Y. Kim, Y. Jang, H. Jeong, M. Reed, and T. Lee, Nature **462**, 1039 (2009).